

Synthetic aperture radar interferometry coherence analysis over Katmai volcano group, Alaska

Zhong Lu

Raytheon STX Corporation, USGS/EROS Data Center, Sioux Falls, South Dakota

Jeffrey T. Freymueller

Geophysical Institute, University of Alaska, Fairbanks

Abstract. The feasibility of measuring volcanic deformation or monitoring deformation of active volcanoes using space-borne synthetic aperture radar (SAR) interferometry depends on the ability to maintain phase coherence over appropriate time intervals. Using ERS 1 C band ($\lambda = 5.66$ cm) SAR imagery, we studied the seasonal and temporal changes of the interferometric SAR coherence for fresh lava, weathered lava, tephra with weak water reworking, tephra with strong water reworking, and fluvial deposits representing the range of typical volcanic surface materials in the Katmai volcano group, Alaska. For interferograms based on two passes with 35 days separation taken during the same summer season, we found that coherence increases after early June, reaches a peak between the middle of July and the middle of September, and finally decreases until the middle of November when coherence is completely lost for all five sites. Fresh lava has the highest coherence, followed by either weathered lava or fluvial deposits. These surfaces maintain relatively high levels of coherence for periods up to the length of the summer season. Coherence degrades more rapidly with time for surfaces covered with tephra. For images taken in different summers, only the lavas maintained coherence well enough to provide useful interferometric images, but we found only a small reduction in coherence after the first year for surfaces with lava. Measurement of volcanic deformation is possible using summer images spaced a few years apart, as long as the surface is dominated by lavas. Our studies suggest that in order to make volcanic monitoring feasible along the Aleutian arc or other regions with similar climatic conditions, observation intervals of the satellite with C band SAR should be at least every month from July through September, every week during the late spring/early summer or late fall, and every 2-3 days during the winter.

1. Introduction

Synthetic aperture radar (SAR) interferometry has been used extensively in recent years to measure ground surface deformation associated with earthquake displacements [e.g., *Massonnet et al.*, 1993; *Murakami et al.*, 1996; *Peltzer and Rosen*, 1995; *Zebker et al.*, 1994a], volcanic activity [*Massonnet et al.*, 1995; *Lu et al.*, 1997; *Rosen et al.*, 1996; *Thatcher and Massonnet*, 1997], glacial ice movement [e.g., *Goldstein et al.*, 1993; *Joughin et al.*, 1996; *Kwok and Fahnestock*, 1996; *Rignot et al.*, 1997], and land surface subsidence [*Massonnet et al.*, 1997]. Repeat-pass interferometry uses the phase difference of the radar returns in two SAR images, acquired at different times by the same antenna or tandem antennas, to construct an interferogram for the analysis of ground surface deformation.

SAR interferometry has an enormous recognized potential for the study of volcanic deformation and for the monitoring of restless volcanoes because of its extensive spatial coverage and because, in theory, it can be applied without having personnel or instrumentation on the ground in harm's way. In addition, with extensive satellite coverage available, we could have the potential to monitor any restless volcano in the world without having to identify it as a likely candidate for monitoring before observing any signs of unrest. Dedicated SAR missions [e.g., *Hermann*, 1996] are being considered that, among other goals, would make it possible to monitor active volcanoes.

However, the ability of SAR interferometry to measure volcanic deformation signals will depend on the ability to maintain phase coherence on volcanic surface materials over appropriate intervals of time. Most large volcanoes, such as those in the Alaska-Aleutian arc, the Cascade Range, or Central and South America, are covered by lava flows, tephra, and snow and ice fields. Large stratovolcanoes, even in tropical climates, are high enough to have seasonal or permanent snow and ice cover, and the loose surface materials found on these volcanoes are highly

Copyright 1998 by the American Geophysical Union.

Paper number 98JB02410.
0148-0227/98/98JB-02410\$09.00

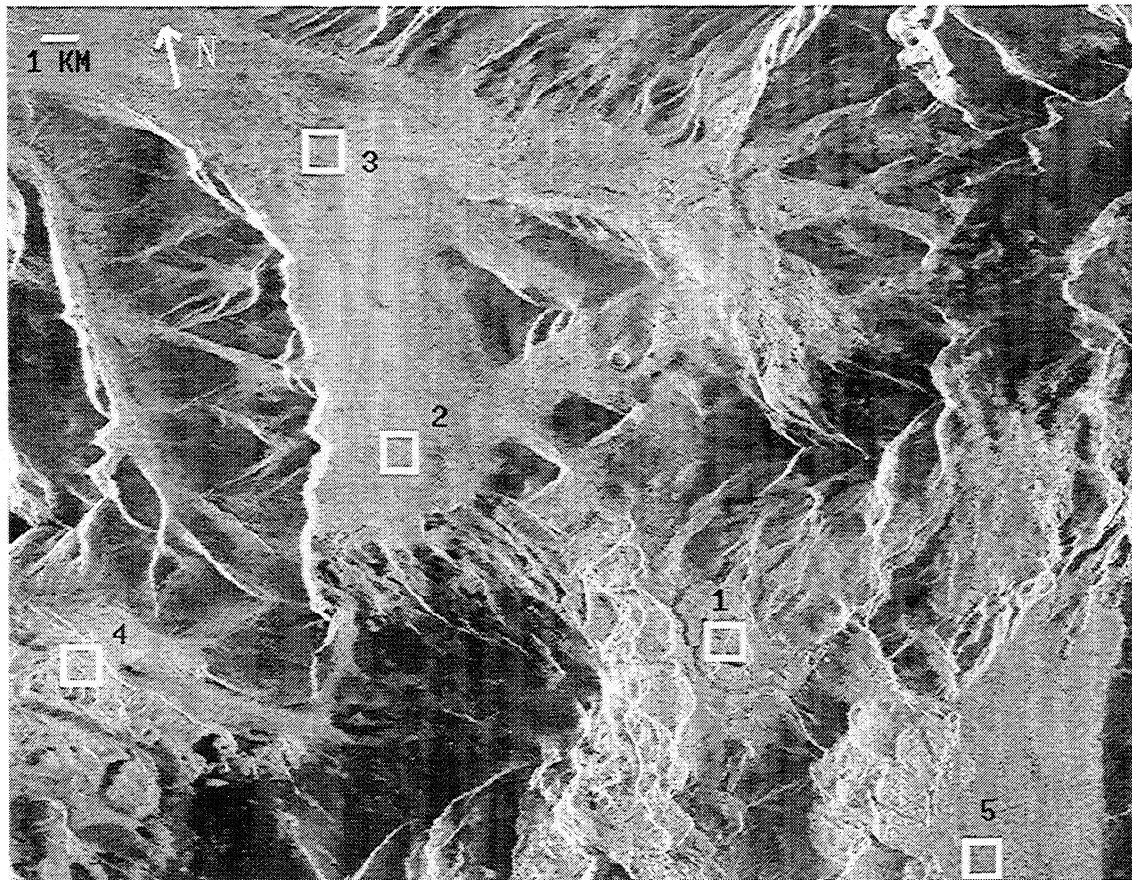


Figure 1. SAR image of Katmai volcano group. Image size is 28 by 22 km. The latitude and longitude of image center are 58.27°N and 155.17°W. The five types of volcanic surface of the test sites (1, fresh lava; 2, tephra with weak water reworking; 3, tephra with strong water reworking; 4, weathered lava; 5, fluvial deposits) are annotated. Average estimate of coherence within each square (1 km by 1 km area) is used for analysis.

susceptible to environmental modification that would reduce phase coherence. Zebker *et al.* [1994b] reported the first interferometric survey of Alaskan volcanoes using data acquired shortly after the launch of ERS 1. They found poor correlation in the predominantly winter season images. In this study, we carried out a systematic study of phase coherence as a function of surface materials, time of year, and time separation between images for an environment typical of many of the world's large stratovolcanoes.

1.1. Phase Coherence

Radar returns must be coherent in order to derive useful information from an interferogram. Coherence is a measure of the variance of phase in an interferogram and can be represented mathematically by a correlation coefficient. The degree of coherent interference of two SAR images depends on the changes of the scattering characteristics of the ground surface between the two radar acquisitions. The coherence of the interferogram will be the highest when the scattering characteristics of the illuminated ground area remain unchanged. Loss of coherence can be caused by physical movement of scattering objects or changes in surface types. Because of the potential for degradation of coherence by environmental effects, the best SAR interferometry deformation results to date have come from

arid regions, such as southern California [e.g., Massonnet *et al.*, 1993; Peltzer and Rosen, 1995; Zebker *et al.*, 1994a]. Theoretical and experimental studies [e.g., Li and Goldstein, 1990; Rodriguez and Martin, 1992; Zebker and Villasenor, 1992; Zebker *et al.*, 1994b] have shown that coherence is determined by (1) the spatial baseline separation of the interferometric pair: the smaller the baseline, the higher the coherence; (2) the time separation of the images: generally the shorter the time interval spanned by the two acquisitions, the higher the coherence (this decorrelation is caused by environmental effects); (3) topographic effects [Werner *et al.*, 1996]; and (4) noise sources such as system thermal noise.

In this paper, we analyzed the SAR interferometric coherence for five types of volcanic surfaces at Katmai volcano group (Figure 1). This systematic study of phase coherence is significant because the extent of phase coherence: (1) partially determines the precision of topographic mapping or ground surface deformation measurement that can be made from an interferogram [e.g., Rodriguez and Martin, 1992]; (2) determines the feasibility of applying interferometric SAR techniques to geophysical studies of volcanoes; (3) provides guidance in the planning of future SAR missions, by showing how often a satellite must pass over a site to make reliable measurements of surface displacement; and (4) could be a key channel for



Plate 1. Composite red-green-blue interferometric coherence map constructed using three representative coherence maps as colors: 35-day coherence as the red channel, 1-year coherence data as the green channel, and 2-year coherence data as the blue channel. The image has the same dimensions as Figure 1. Green and blue colors represent regions that maintain good coherence over more than 1 year, which probably represent areas covered by lavas.

image classification for land and forest mapping [e.g., Wegmüller and Werner, 1995, 1997; Zebker *et al.*, 1996].

2. Analysis

Images recorded by the European Space Agency's ERS 1 SAR were used for this study. ERS 1 is a C band radar with wavelength $\lambda = 5.66$ cm. All the images were acquired during descending passes where the satellite travels approximately from north to south and looks down to the west at 23° from vertical, and when the satellite was in either 3-day or 35-day repeat cycle modes. The image acquisition time is about 2126 UT, or 1:26 p.m. Alaska daylight time. We evaluated the phase coherence of 78 interferograms using 45 ERS 1 complex images for the area shown in Figure 1, with time separations ranging from 3 days to 3 years. Orbit numbers and acquisition dates of the image pairs are shown in Table 1. We selected five specific 1 km by 1 km areas where the surface material is known on the basis of geological experience in the field (J. Eichelberger, personal communication, 1996). The target areas were selected prior to forming the interferograms. The five types of volcanic surface materials examined, and the latitude, longitude, and elevation of the five test sites (Figure 1) are as follows: fresh lava (latitude: 58.20°N , longitude: 155.13°W , elevation: 579 m); tephra with weak

water reworking (latitude: 58.27°N , longitude: 155.24°W , elevation: 610 m); tephra with strong water reworking (latitude: 58.37°N , longitude: 155.28°W , elevation: 428 m); weathered lava (latitude: 58.22°N , longitude: 155.27°W , elevation: 686 m); fluvial deposits (latitude: 58.15°N , longitude: 155.01°W , elevation: 153 m).

A final data set of the best interferograms was selected on the basis of two criteria: (1) the baseline separation was smaller than 500 m (Table 1), and (2) coherence was found somewhere on the image (i.e., if an interferogram did not show any coherent fringes anywhere on the image, it was excluded). We did not give preference to interferograms that showed coherence in one or more of our target areas. Our final data set consisted of 59 interferograms that met the above two criteria (Table 1).

We computed a correlation coefficient for each site for each pair of images, using the following equation,

$$\rho = \frac{\left| \sum_{i=1}^{20} (a_i \times b_i^*) \right|}{\sqrt{\sum_{i=1}^{20} (a_i \times a_i^*) \sum_{i=1}^{20} (b_i \times b_i^*)}} \quad (1)$$

where a_i and b_i are complex-valued pixels in the two images, and the asterisk means complex conjugation. In the

Table 1. Interferometric Data Acquisition Parameters

orbit 1	orbit 2	date 1	date 2	B_{\perp}	B_{\parallel}
00814	00857	1991:254	1991:257	258	-122
00814	00943	1991:254	1991:263	-273	11
00814	01029	1991:254	1991:269	-336	157
00814	01459	1991:254	1991:299	-277	128
00814	01502	1991:254	1991:302	-213	51
00943	01029	1991:263	1991:269	-63	146
00943	01416	1991:263	1991:296	-439	135
00943	01459	1991:263	1991:299	-3	117
00943	01502	1991:263	1991:302	61	40
01029	01416	1991:269	1991:296	-370	-11
01029	01459	1991:269	1991:299	59	-29
01029	01502	1991:269	1991:302	123	-106
01330	01760	1991:290	1991:320	-200	204
01330	02061	1991:290	1991:341	-233	196
01416	01459	1991:296	1991:299	429	19
01459	01502	1991:299	1991:302	64	-77
01760	02061	1991:320	1991:341	-33	-8
01846	01932	1991:326	1991:332	114	-64
01846	01975	1991:326	1991:335	-267	63
04654	05155	1992:157	1992:192	-345	147
04654	06157	1992:157	1992:262	401	-202
04654	10666	1992:157	1993:211	2	-15
04654	11167	1992:157	1993:246	132	-13
04654	11668	1992:157	1993:281	210	-3
04654	21531	1992:157	1995:239	74	-41
05155	05656	1992:192	1992:227	-218	138
05155	10165	1992:192	1993:176	94	-63
05155	10666	1992:192	1993:211	349	-162
05427	10938	1992:211	1993:230	177	-40
05427	20300	1992:211	1995:153	-39	22
05427	21302	1992:211	1995:223	-263	115
05656	10165	1992:227	1993:176	312	-201
06157	11167	1992:262	1993:246	-296	195
06157	11668	1992:262	1993:281	-191	199
06157	21030	1992:262	1995:204	284	-159

Table 1. (continued)

orbit 1	orbit 2	date 1	date 2	B_{\perp}	B_{\parallel}
09936	10437	1993:160	1993:195	101	-43
09936	10938	1993:160	1993:230	-282	141
10165	10666	1993:176	1993:211	252	-98
10165	11167	1993:176	1993:246	356	-91
10165	11668	1993:176	1993:281	460	-87
10165	20529	1993:176	1995:169	63	-36
10165	21531	1993:176	1995:239	324	-125
10666	11167	1993:211	1993:246	113	7
10666	11668	1993:211	1993:281	208	11
10666	20529	1993:211	1995:169	-189	63
10666	21030	1993:211	1995:204	-115	28
10666	21531	1993:211	1995:239	72	-27
10938	21302	1993:230	1995:223	-440	155
11167	11668	1993:246	1993:281	105	4
11167	20529	1993:246	1995:169	308	52
11167	21030	1993:246	1995:204	-11	36
11167	21531	1993:246	1995:239	-31	-34
11439	21302	1993:265	1995:223	355	-90
11668	21030	1993:281	1995:204	93	40
11668	21531	1993:281	1995:239	136	38
20300	21302	1995:153	1995:223	-224	93
20529	21030	1995:169	1995:204	305	-91
20529	21531	1995:169	1995:239	262	-89
21030	21531	1995:204	1995:239	-39	2

Acquisition date is given by year and Julian day; B_{\perp} is baseline component perpendicular to look direction, in meters; B_{\parallel} is baseline component parallel to look direction, in meters.

original SAR image, an area of 1 km by 1 km represents 50 pixels (20 m pixel spacing) in the across-track direction and 250 pixels (4 m pixel spacing) in the along-track direction. Interferogram and correlation coefficient (based on (1)) were generated with 2 looks in the across-track direction and 10 looks in the along-track direction. This results in 625 (25 pixels in the across-track direction and 25 pixels in the along-track direction) independent estimates of ρ , each averaged over an area of 40 m by 40 m. The 625 samples of ρ within each test area were averaged to give an estimate of ρ for each target area (1 km by 1 km). All five of our target areas are relatively flat, so

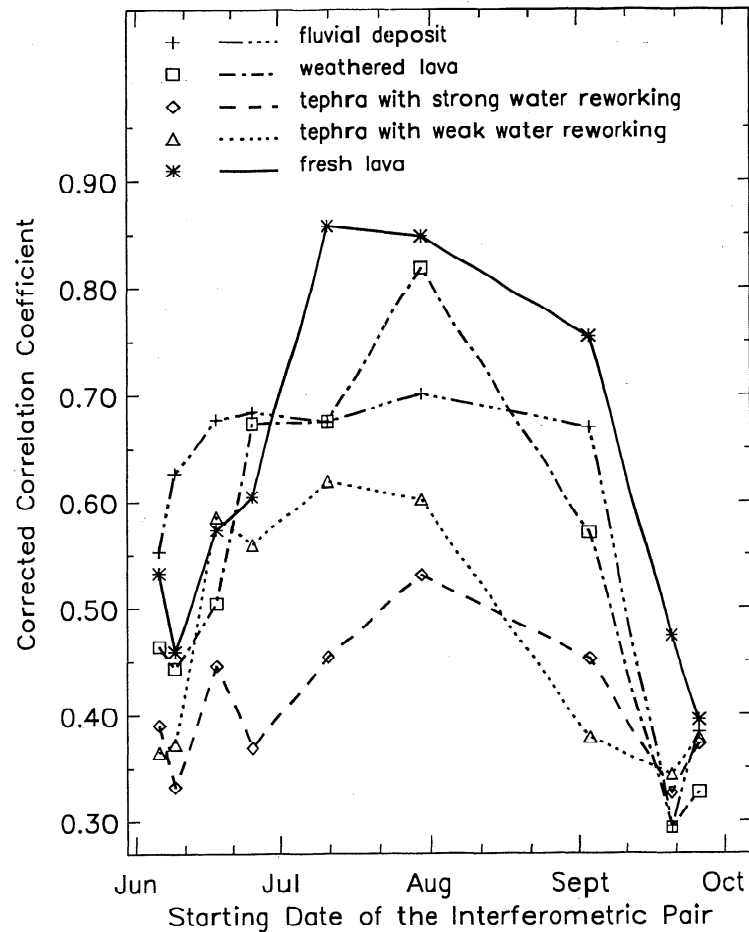


Figure 2. Corrected correlation coefficient as a function of starting date of the image pair. Time intervals of the interferometric pairs are fixed to be 35 days.

the topographic effect on ρ is minimized. *Fujiwara et al.* [1998] used a similar method to characterize phase coherence for JERS 1 images from the Izu peninsula, Japan, with time separations of up to several months.

Because ρ depends strongly on the baseline separation, we correct for the loss of coherence caused by increasing baseline separation by using the linear equation proposed by *Zebker and Villasenor* [1992]. This is based on the theoretical calculation that ρ should be equal to 1 (in the absence of noise) at a zero baseline and drop to zero at a critical baseline separation (about 1100 m for ERS 1) if loss of coherence caused by environmental effects is assumed to be zero. *Fujiwara et al.* [1998] found that this theoretical relationship holds well except in regions of high relief. We assumed that the effect of baseline separation could be modeled as a multiplicative factor and then corrected the observed ρ to a value at zero baseline length. The corrected ρ is then a function of the surface material and environmental effects. We studied the dependence of phase coherence on the starting date of the interferogram and the time interval spanned by the two images used to form the interferogram.

2.1. Seasonal Variations in Coherence

Low-lying areas within the Katmai volcano group are covered with seasonal snow for more than 6 months each

year, and high areas are free of snow cover for 2 or 3 months a year at most. In addition to the effect of the snow itself, which will change the phase of the radar signals, other seasonal effects, such as annual snow melting and freezing/thawing of the ground surface, can make for significant changes in the radar scattering properties. As a result, it is reasonable to expect a systematic relationship between phase coherence and the starting date of the interferogram, given a constant separation time.

To test for the presence of such a relationship, we compared the correlation coefficient ρ for nine interferograms with exactly 35 days separation (Figure 2). The correlation coefficients were adjusted for the effect of baseline separation, as described above; the time axis refers to the time of the first satellite pass. The phase coherence begins to increase from early June and peaks between the middle of July and the middle of September. After the middle of September the correlation coefficient decreases, dropping to a stage of complete decorrelation ($\rho < 0.3$) by the end of October or early November. The period of highest coherence corresponds to the short Arctic summer, when little or no snow is present on the ground.

All of the surface materials tested show a similar relationship between coherence and starting date, with some surface materials giving better coherence than others, regardless of the starting date. Fresh lava had the highest

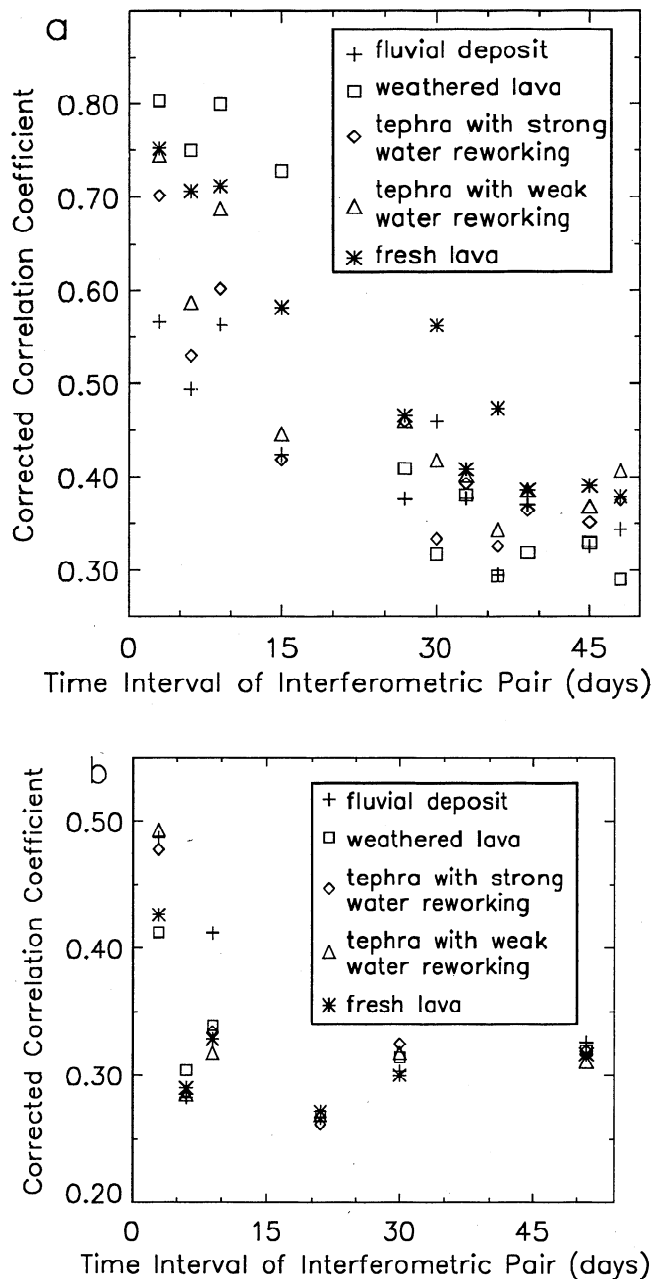


Figure 3. Loss of coherence as a function of time in (a) later fall and (b) in winter. The starting date of the interferometric pair is the middle of September for Figure 3a, and the middle of November for Figure 3b.

coherence among the five types of volcanic surfaces, followed by weathered lava and fluvial deposits, and finally tephtras. In general, tephtras with weak water reworking have higher coherence than those with strong water reworking. It is not surprising that fresh or weathered lavas maintain coherence better than looser materials, but it is somewhat surprising that the fluvial deposits show coherence that is nearly as good as some of the lavas. One possible explanation is that the fluvial deposits may contain boulders or cobbles that are strong scatterers and that these scatterers will not move or otherwise change their radar backscattering characteristics during the Arctic summer. Fine-grained materials such as tephtras are easily modified

by wind or water and may change their radar backscatter characteristics significantly as their water content varies.

We examined the seasonal dropoff in coherence for images collected after the middle of September when the ERS 1 satellite was in the 3-day repeat cycle stage. In Figure 3a we show the correlation coefficient ρ , corrected for baseline separation, as a function of the time interval spanned by the interferogram. The first image was collected in mid-September. For all surface types, there is a steady decrease in coherence with time after mid-September, from a ρ of 0.75 to a ρ of less than 0.4 at 30 days (mid-October). After 30 days, there is no significant difference of the correlation coefficients among the five surface types (Figure 3a); we suggest that the lack of such a difference indicates that snow, ice, freezing, or thawing on the ground is the most likely explanation for reduction in coherence. After ~ 35 days, the correlation coefficient is much lower than it would be during the summer (compare the correlation coefficient values in Figures 2 and 3a). Weather data for the specific times of the satellite passes are not available in this unpopulated area, but snow can fall at any time of the year there, and snow on the ground becomes increasingly common after mid-September.

A more rapid dropoff in coherence is found for interferograms starting around the beginning of November (Figure 3b). At this time of year, the coherence of interferograms spanning more than 3 days is very low, indicating almost complete decorrelation within 6 days. Once again the surface types cannot be distinguished, and we suggest that changes in snow and ice cover are the most likely cause of decorrelation.

2.2. Coherence as a Function of Time Interval Spanned by the Interferogram

Past studies have shown that, in general, a degradation of phase coherence occurs with increasing time between the satellite passes [e.g., Zebker and Villasenor, 1992; Fujiwara et al., 1998; Zebker et al., 1994b]. To quantify the effect for different volcanic surfaces, we selected a set of interferograms with approximately the same starting dates to minimize the effect of the seasonal variations in coherence described above. Our data set contains seven suitable interferograms with starting dates ranging from Julian day 192 to 211 (mid to late July) and with time intervals ranging from 35 days to 3 years. All satellite passes used to construct these interferograms occurred during the summer period of highest coherence.

Figure 4 shows that phase coherence decays with increasing time separation for all surface types. A comparison of the five surface types shows similar results to those obtained with the shorter term interferograms used in the previous section, with lavas showing better results than tephtras. The fluvial deposits, however, fare much worse over the long term than would be predicted on the basis of interferograms spanning no more than a few months. With a time separation of 1 year, the coherence of the fluvial deposits is no better than for the tephtras, but over periods of weeks or months the fluvial deposits show coherence similar to the lavas. One possible explanation is that the scattering objects in the fluvial deposits are easily moved by the ice and snow or by the spring melt, which changes their radar backscattering characteristics from year to year.

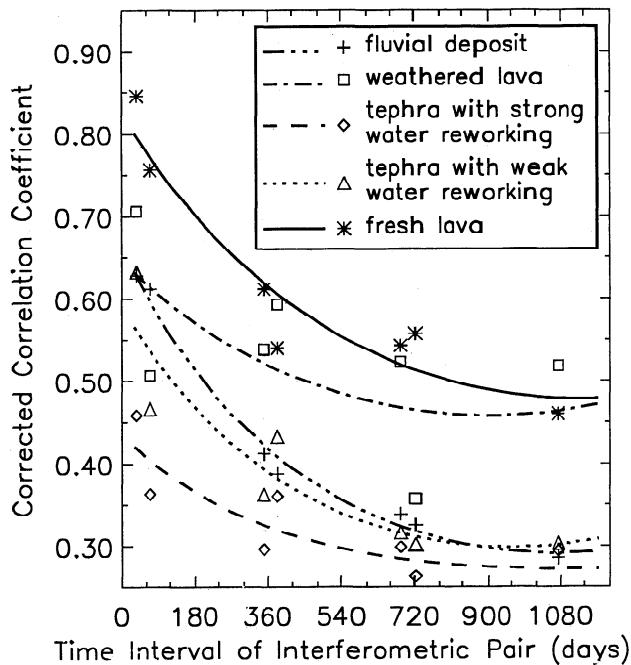


Figure 4. Long-term decay of coherence for five types of volcanic surface. Only summer images are used here. The curves are the exponential fit to the observed coherence. Time constants are of the order of about 2 years.

We constructed a composite image from three representative interferometric coherence maps with time separations of 35 days, 1 year, and 2 years (Plate 1). The coherence is computed over 40 by 40 m areas for the entire image. We use the 35 day interferometric coherence as the red channel, the 1 year interferometric coherence as the green channel, and the 2 year interferometric coherence as the blue channel, with each pixel's color determined by the appropriate values of ρ . The lava flows (greenish and bluish colors) have good coherence at 1 to 2 year time interval, and tephra and fluvial deposits (reddish colors) only have good coherence for the 35 day separation. Using image classification techniques, lava flows can be distinguished from tephra by comparing interferometric coherence maps of different time windows.

3. Discussions and Conclusions

For all five sites we found that coherence increases after early June, reaches a peak between the middle of July and the middle of September, and finally decreases until the middle of November when coherence is completely lost. We interpret this observation to mean that coherence is highest during the Arctic summer, when the ground is free of snow and ice, and when the reworking and water saturation caused by the spring melt has passed.

For interferograms based on two passes taken during the same summer season, fresh lava has the highest coherence, followed by either weathered lava or fluvial deposits. These surfaces maintain relatively high levels of coherence for periods up to the length of the summer season. Coherence degrades rapidly with time for surfaces covered with tephra, and presumably, other loose materials behave similarly. Fresh lavas in the Katmai group are blocky and

rough and are not easily modified by wind or water. This makes the radar return signals very strong and the interferometric coherence very high. The surface of weathered lava or fluvial deposits is not as rough as fresh lava, and more loose materials are present, resulting in generally lower coherence. We suggest that the excellent performance of the site with fluvial deposits may be due to the presence of small boulders or cobbles that provide strong radar return signals. However, this site had very low coherence in interferograms based on two satellite passes taken in different summer seasons, which we interpret is due to motion of the scatterers caused by ice or the spring melt.

The coherence as a function of time interval for interferometric SAR images acquired during the summer can be described as an approximately exponential decrease in correlation coefficient with time (Figure 4). The best fitting exponential decay curve for the fresh lava has a time constant of several years. However, we do not believe that a simple exponential function is adequate to describe our results. In Figure 4, note that the dropoff in coherence for fresh lava goes from values around 0.8 with a time separation of 1-2 months to 0.5-0.6 for time separations of 1 to 3 years. There is a significant drop in correlation coefficient from a separation of a few months to a separation of 1 year. However, the drop in coherence for separations of 2 and 3 years is much smaller. We suggest that multiple processes, each acting with a different exponential timescale, would better fit the data.

The complete loss of interferometric coherence at $\rho \sim 0.3$ (Figures 3b and 4) shows a probable bias in the correlation coefficient at low correlation values [Wegmüller and Werner, 1995; Zebker et al., 1996]. Correlation coefficients based on (1) are both statistical and biased [Wegmüller and Werner, 1995; Zebker et al., 1996]. If there is any noise in the measurement, (1) always gives a greater value than the true result [Wegmüller and Werner, 1995; Zebker et al., 1996]. For medium and high correlation values, the bias is negligible, but at lower values it is significant [Zebker et al., 1996]. In our study, the average correlation coefficient almost never drops below 0.3, even when a region is almost completely incoherent. Both Wegmüller and Werner [1995] and Zebker et al. [1996] suggested averaging over a large number of complex-valued pixels to obtain a better estimate of the correlation coefficient, but at the cost of spatial resolution. Care must be taken when comparing the correlation coefficients (especially $\rho < 0.3$) from this study with others that used different averaging schemes.

Our results are very encouraging, since they show that even in severe environments like Arctic volcanoes, SAR interferometry can obtain acceptable phase coherence for at least some volcanic surface materials for time separations of multiples of a few years. Wherever relatively fresh lava is found, it is reasonable to expect that interferograms spanning up to a few years can be formed and potentially could be used to measure long-term deformation. Unfortunately, the tephra and fluvial deposit sites have decorrelated after only 1 year to the point that meaningful phase coherence is entirely lost. Other types of volcanic surface materials, such as well-developed soils, were not tested by this study. We have also formed interferograms for Akutan volcano, on Akutan island in the

Aleutian chain, using passes separated by a few months up to 3 years. These interferograms show large regions of coherence, more than 35 percent of the island even for a 3-year separation, suggesting that many volcanic surfaces not covered by fresh loose material like recently erupted tephra can produce usable interferograms.

Our observations have significant implications for volcanic deformation studies and for monitoring volcanic hazards using satellite radar interferometry. Good coherence at C band can be maintained for at least 3 years on some volcanic surfaces, which makes studies of significant deformation events possible even when the only available images were taken a few years apart, as long as a significant area covered by lava is present. However, the rapid loss of coherence at C band for other surface materials and the short window during which interferometric measurements are possible pose difficulties from a monitoring standpoint. To obtain the most usable results for reliably monitoring restless volcanoes in the Alaska-Aleutian arc or others with similar climates, satellite passes must be made at least every month from July through September, every week during the late spring/early summer or late fall, and every 2-3 days during the winter. Seasonal or permanent snow and ice are found at high elevations on many large stratovolcanoes worldwide; we hypothesize that similar results will be found for high-elevation areas of volcanoes at lower latitudes. The spatial baseline length should be as small as possible to reduce the decorrelation effects. Because coherence is lost more rapidly for C band observations than for, say, L band ($\lambda \sim 24$ cm) [e.g., Rosen *et al.*, 1996], observation intervals for an L band SAR volcanic monitoring system could be longer than those we have suggested for C band SAR.

Acknowledgments. We thank Barry Parsons, Paul Rosen, and Dave Rothery for their helpful and constructive comments and reviews. We thank John Eichelberger, Rob Fatland, Shusun Li, and Dave Meyer for contributions made to this research. Internal U.S. Geological Survey reviews by Dean Gesch and Grant Mah are appreciated. This research was performed with the support from NASA (NAG5-4396) and under the U.S. Geological Survey contract 1434-CR-97-CN-40274.

References

- Fujiwara, S., P. A. Rosen, M. Tobita, and M. Murakami, Crustal deformation measurements using repeat-pass JERS-1 synthetic aperture radar interferometry near the Izu Peninsula, Japan, *J. Geophys. Res.*, **103**, 2411-2426, 1998.
- Goldstein, R. M., H. Engelhardt, B. Kamb, and R. M. Frolich, Satellite radar interferometry for monitoring ice sheet motion: Application to an Antarctic ice stream, *Science*, **262**, 1525-1530, 1993.
- Hermann, J., Study on dedicated SAR interferometry mission, paper presented at Fringe 96 Workshop, European Space Agency, Zurich, Switzerland, Sept. 30 - Oct. 2, 1996.
- Joughin, I., and S. Tulaczyk, M. Fahnestock, and R. Kwok, A mini-surge on the Ryder Glacier, Greenland, observed by satellite radar interferometry, *Science*, **274**, 228-230, 1996.
- Kwok, R., and M. A. Fahnestock, Ice sheet motion and topography from radar interferometry, *IEEE Trans. Geosci. Remote Sens.*, **34**, 189-200, 1996.
- Li, F. K., and R. M. Goldstein, Studies of multibaseline spaceborne interferometric synthetic aperture radars, *IEEE Trans. Geosci. Remote Sens.*, **28**, 88-96, 1990.
- Lu, Z., R. Fatland, M. Wyss, S. Li, J. Eichelberger, K. Dean, and J. Freymueller, Deformation of New Trident volcano measured by ERS-1 SAR interferometry, Katmai National Park, Alaska, *Geophys. Res. Lett.*, **24**, 695-698, 1997.
- Massonnet, D., M. Rossi, C. Carmona, F. Adragna, G. Peltzer, K. Feigl, and T. Rabaute, The displacement field of the Landers earthquake mapped by radar interferometry, *Nature*, **364**, 138-142, 1993.
- Massonnet, D., P. Briole, and A. Arnaud, Deflation of Mount Etna monitored by spaceborne radar interferometry, *Nature*, **375**, 567-570, 1995.
- Massonnet, D., T. Holzer, and H. Vadon, Land subsidence caused by the East mesa geothermal field, California, observed using SAR interferometry, *Geophys. Res. Lett.*, **24**, 901-904, 1997.
- Murakami, M., M. Tobita, S. Fujiwara, T. Saito, and H. Masaharu, Coseismic crustal deformations of 1994 Northridge California earthquake detected by interferometric JERS-1 SAR, *J. Geophys. Res.*, **101**, 8605-8614, 1996.
- Peltzer, G., and P. Rosen, Surface displacement of the 17 May 1993 Eureka Valley, California, earthquake observed by SAR interferometry, *Science*, **268**, 1333-1336, 1995.
- Rignot, E. J., S. P. Gogineni, W. B. Krabill, and S. Ekholm, North and northeast Greenland ice discharge from satellite radar interferometry, *Science*, **276**, 934-937, 1997.
- Rodriguez, E., and J. M. Martin, Theory and design of interferometric synthetic aperture radars, *Proc. IEEE*, **139**, 147-159, 1992.
- Rosen, P., S. Hensley, H. Zebker, F. H. Webb, and E. J. Fielding, Surface deformation and coherence measurements of Kilauea volcano, Hawaii, from SIR-C radar interferometry, *J. Geophys. Res.*, **101**, 23109-23125, 1996.
- Thatcher, W., and D. Massonnet, Crustal deformation at Long Valley Caldera, eastern California, 1992-1996, inferred from satellite radar interferometry, *Geophys. Res. Lett.*, **24**, 2519-2522, 1997.
- Werner, C., S. Hensley, and P. Rosen, Application of the interferometric correlation coefficient for measurement of surface change (abstract), *Eos Trans. AGU*, **77**, (46), Fall Meet. Suppl., F49, 1996.
- Wegmüller, U., and C. L. Werner, SAR interferometric signatures of forest, *IEEE Trans. Geosci. Remote Sens.*, **33**, 1153-1161, 1995.
- Wegmüller, U., and C. L. Werner, Retrieval of vegetation parameters with SAR interferometry, *IEEE Trans. Geosci. Remote Sens.*, **35**, 18-24, 1997.
- Zebker, H. A., and J. Villasenor, Decorrelation in interferometric radar echoes, *IEEE Trans. Geosci. Remote Sens.*, **30**, 950-959, 1992.
- Zebker, H. A., P. A. Rosen, R. M. Goldstein, A. Gabriel, and C. L. Werner, On the derivation of coseismic displacement fields using differential radar interferometry: The Landers earthquake, *J. Geophys. Res.*, **99**, 19617-19634, 1994a.
- Zebker, H. A., C. L. Werner, P. L. Rosen, and S. Hensley, Accuracy of topographic maps derived from ERS-1 interferometric radar, *IEEE Trans. Geosci. Remote Sens.*, **32**, 823-836, 1994b.
- Zebker, H., P. Rosen, S. Hensley, and P. Mousinis-Mark, Analysis of active lava flows on Kilauea volcano, Hawaii, using SIR-C radar correlation measurements, *Geology*, **24**, 495-498, 1996.

J. T. Freymueller, Geophysical Institute, University of Alaska, Fairbanks, AK 99775. (e-mail: jeff@giseis.alaska.edu)
Z. Lu, Raytheon STX Corporation, USGS/EROS Data Center, Sioux Falls, SD 57198. (e-mail: lu@edcmail.cr.usgs.gov)

(Received March 10, 1998; revised May 29, 1998; accepted July 16, 1998.)